

# Continuum limit of the quasi-PDF operator using chiral fermion



Kuan Zhang,<sup>1,2</sup> Yuan-Yuan Li,<sup>3</sup> Yi-Kai Huo,<sup>4</sup> Peng Sun,<sup>3,\*</sup> and Yi-Bo Yang<sup>2,5,6,†</sup>

( $\chi$ QCD Collaboration)

<sup>1</sup>*University of Chinese Academy of Sciences, School of Physical Sciences, Beijing 100049, China*

<sup>2</sup>*CAS Key Laboratory of Theoretical Physics, Institute of Theoretical Physics, Chinese Academy of Sciences, Beijing 100190, China*

<sup>3</sup>*Nanjing Normal University, Nanjing, Jiangsu, 210023, China*

<sup>4</sup>*Physics Department, Columbia University, New York, NY 10027*

<sup>5</sup>*School of Fundamental Physics and Mathematical Sciences,*

*Hangzhou Institute for Advanced Study, UCAS, Hangzhou 310024, China*

<sup>6</sup>*International Centre for Theoretical Physics Asia-Pacific, Beijing/Hangzhou, China*

(Dated: February 7, 2022)

Non-perturbative renormalization using the regularization independent momentum subtraction (RI/MOM) scheme has achieved great success in dealing with local operators under the lattice regularization, while a high accuracy and systematic examination on its validity of the non-local operator likes the quasi-PDF operator, such as the quark bi-linear operator with Wilson link which suffers from the linear divergence, is still absent. In this work, we compute the pion unpolarized quasi-PDF matrix element in the rest frame at 11 lattice spacings from 0.032 to 0.121 fm, using the discretized fermion actions with or without additive chiral symmetry breaking, on 3 kinds of dynamical gauge ensembles. The result shows that RI/MOM renormalization cancels all the linear divergence for the chiral fermion at least up to Wilson link length  $z \sim 1.2$  fm. But in the case of the clover action which has additive chiral symmetry breaking, there is still a conspicuous residual linear divergence when the lattice spacing is much smaller than 0.1 fm.

**Introduction:** The intrinsic properties of nucleon and also nuclear, is at the center of the non-perturbative QCD study. Based on the fundamental theory, the nucleon collision cross sections can be factorized into perturbative calculable short distance kernel and universal nucleon parton distribution functions (PDFs). PDF describes the energy distribution of given parton inside a high-momentum nucleon, and it has several extensions to describe the 3D picture of nucleon, such as transverse momentum dependent PDF, generalized PDF and so on. One can use them to describe the nucleon and nuclear properties, such as the gluon and sea quark contributions to the nucleon mass, momentum and spin, and also nuclear medium effects based on the difference between the nucleon and nuclear PDFs.

Currently, PDFs are mainly determined phenomenologically with the global analysis of the experimental data. The first principle prediction of PDF was not possible with lattice QCD calculations, since the light-cone gauge link in the PDF definition can not be implement on a Euclidean lattice. The Large Momentum Effective theory (LaMET) suggests a quasi-PDF operator  $O_\Gamma(z) = \bar{\psi}(0)\Gamma U(0,z)\psi(z)$  with spatial gauge link  $U(0,z) = \exp(-ig \int_0^z dz' A_z(z'))$ , and connects its renormalized nucleon matrix element to PDF through the fac-

torization theorem [1–5]. But the bare  $O_\Gamma(z)$  under lattice regularizations looks like

$$O_\Gamma(z) = \Gamma(1 + g^2(\gamma \log(p^2 a^2) - m_{-1} \frac{z}{a}) + \dots), \quad (1)$$

at 1-loop level [6] with lattice spacing  $a$ , and then can deviate from the tree level value exponentially at either large  $z$  or small  $a$  when higher order effects are summed over. Thus a non-perturbative renormalization with accurate cancellation on the linear divergence is essential for the quasi-PDF, to ensure the existence of a finite continuum limit.

RI/MOM scheme has been proposed for more than 20 years [7], and has been applied to various quark and gluon local operators. Since the theoretical studies show that the quasi-PDF operator is multiplicative renormalizable [8–11] in the continuum, there are many studies to apply RI/MOM renormalization to the quasi-PDF operator, starting from the investigations in Refs. [6, 11–14]. The recent studies using multiple lattice spacings [15, 16] studied the lattice spacing dependence on the quasi-PDF, however the precision of their data were not enough to justify whether the dependence is a discretization error or not.

In this work, we study the RI/MOM renormalized pion quasi-PDF matrix element in the rest frame, on 11 lattice spacings from 0.032 to 0.121 fm with different quark and gluon actions. The result shows that the linear divergences can be cancelled effectively and the lattice spacing dependence is at 1% level with the chiral fermion. On the

\* 06260@njnu.edu.cn

† ybyang@itp.ac.cn

other hand, the residual linear divergence is still clearly visible using the clover fermion, especially when the lattice spacing is much smaller than 0.1 fm.

**Numerical setup:** When we consider the quasi PDF nucleon matrix element in the moving frame, the gap  $\delta m$  between the ground and first excited states can decrease significantly with large momentum and then a large source/sink separation  $t_{\text{sep}}$  is required to eliminate the excited state contaminations. At the same time, the signal to noise ratio also decreases exponentially on  $t_{\text{sep}}$ , and then it decreases our ability to identify the lattice spacing dependence from the data with large statistical and/or systematic uncertainties.

In order to avoid the defects above, the pion matrix element in the rest frame can be a better choice. It is known that the first excited state of pion is higher than 1GeV, and the signal to noise ratio is almost independent to  $t_{\text{sep}}$ . Thus we can set the  $t_{\text{sep}}$  to be one half of the lattice length  $T$  along the temporal direction which can be larger than 2 fm, and then obtain the ground state matrix element  $h_\pi = \langle \pi | O_{\gamma_t}(z) | \pi \rangle$  with high accuracy:

$$\begin{aligned} R_\pi(T/2, t, z; a) &= \frac{\langle O_\pi(T/2) \sum_{\vec{x}} (O_\Gamma(z; (\vec{x}, t)) + O_\Gamma(z; (\vec{x}, T-t))) O_\pi^\dagger(0) \rangle}{\langle O_\pi(T/2) O_\pi^\dagger(0) \rangle} \\ &= h_{\pi, \Gamma}(z) + \mathcal{O}(e^{-\delta m t}) + \mathcal{O}(e^{-\delta m (T/2-t)}) + \mathcal{O}(e^{-\delta m T/2}), \end{aligned} \quad (2)$$

where  $O_\pi$  is the pion interpolation field. Note that the denominator includes both the forward and backward two point functions needed by the two terms in the numerator, due to the loop around effect in the temporal direction.

In the RI/MOM renormalization, we define the normalized renormalization constant as [17],

$$Z_{\gamma_t}(z, \mu) = \frac{\text{Tr}[\gamma_t \langle q(p) | O_{\gamma_t}(z) | q(p) \rangle]}{\text{Tr}[\gamma_t \langle q(p) | O_{\gamma_t}(0) | q(p) \rangle]} \Big|_{p^2 = -\mu^2, p_z = p_t = 0}, \quad (3)$$

where  $|q(p)\rangle$  is the off-shell quark state with external momentum  $p$ . When the Landau gauge fixed volume( $V$ ) source [13] is used in the calculation, the statical uncertainty is suppressed by a factor  $1/\sqrt{V}$  comparing to the point source case. By eliminating the  $z$  and  $t$  components of  $p$ , the matrix element is free of the operator mixing and avoids the related systematic uncertainties.

Then we can apply  $Z_{\gamma_t}$  on the bare pion matrix element  $h_{\pi, \gamma_t}(z)$  to obtain the non-perturbative renormalized and normalized matrix element at given RI/MOM scale  $\mu$ ,

$$h_{\pi, \gamma_t}^r(z, \mu) = Z_{\gamma_t}(z, \mu) \frac{h_{\pi, \gamma_t}(z)}{h_{\pi, \gamma_t}(0)}. \quad (4)$$

The joint effect of the normalizations on both quark and pion matrix elements is equivalent to the original RI/MOM definition which uses the conserved vector current to define the quark self energy.

In order to check if the linear divergence is relate to the fermion action definition, we consider two kinds of fermion actions in this work: the clover and overlap actions. It is relatively cheap to calculate the quark propagator for the clover action and it is widely used in the quasi-pdf calculations, and the overlap propagator is much more expensive but it conserves chiral symmetry.

The clover fermion action is defined by the Wilson action

$$\begin{aligned} S_q^w &= \sum_{x,y} \bar{\psi}(x) D_w(m_q^w; x, y) \psi(y), \\ D_w(m_q^w; x, y) &= \frac{1 - \gamma_\mu}{2a} U(x, x + \hat{n}_\mu) \delta_{x+\hat{n}_\mu, y} \\ &+ \frac{1 + \gamma_\mu}{2a} U(x, x - \hat{n}_\mu) \delta_{x-\hat{n}_\mu, y} - \left(\frac{4}{a} + m_q^w\right) \delta_{x,y}, \end{aligned} \quad (5)$$

with an additional ‘‘clover’’ term,

$$S_q^{\text{clv}} = S_q^w + a c_{\text{sw}} \sum_x \bar{\psi}(x) \sigma_{\mu\nu} F_{\mu\nu}(x) \delta_{x,y} \psi(y), \quad (6)$$

where  $\hat{n}_\mu$  is the unit vector along the  $\mu$  direction,  $m_q^w - m^{\text{cri}}$  is the multiplicative renormalizable bare quark mass, and  $m^{\text{cri}}$  is the bare quark mass which vanishes the pion mass.  $m^{\text{cri}}$  is  $\mathcal{O}(\frac{\alpha_s}{a})$  at the leading order for the Wilson action and always negative, but it can be suppressed to  $\mathcal{O}(\frac{\alpha_s^2}{a})$  (but usually still negative) with a clover coefficient  $c_{\text{sw}} = 1 + \mathcal{O}(\alpha_s)$ . It can be further suppressed by applying the smearing on the gauge link  $U$  and/or tuning  $c_{\text{sw}}$  manually, while it can not exactly vanish due to the random gauge fluctuations.

To eliminate  $m^{\text{cri}}$  accurately, one can use the chiral fermion which satisfies the Ginsburg-Wilson relation  $D_{\text{ov}} \gamma_5 + \gamma_5 D_{\text{ov}} = \frac{a}{\rho} D_{\text{ov}} \gamma_5 D_{\text{ov}}$  [18]. For example, Refs. [19, 20] define the overlap fermion as

$$\begin{aligned} S_q^{\text{ov}} &= \sum_{x,y} \bar{\psi}(x) D_{\text{ov}}(x, y) \psi(y), \quad (7) \\ D_{\text{ov}} &= \rho \left( 1 + \frac{D_w(-\rho)}{\sqrt{D_w^\dagger(-\rho) D_w(-\rho)}} \right), \end{aligned}$$

where  $-\rho$  should be lower than  $m^{\text{cri}}$ , to make  $D_{\text{ov}}$  to be the same as the standard Dirac operator in the continuum limit. The chiral fermion propagator can be further defined through  $D_{\text{ov}}$ ,

$$\frac{1}{D_c + m_q^{\text{ov}}} = \frac{1}{\frac{D_{\text{ov}}}{1 - \frac{1}{2\rho} D_{\text{ov}}} + m_q^{\text{ov}}} = \frac{1 - \frac{1}{2\rho} D_{\text{ov}}}{D_{\text{ov}} + m_q^{\text{ov}} (1 - \frac{1}{2\rho} D_{\text{ov}})}, \quad (8)$$

where  $D_c$  satisfies the relation  $D_c \gamma_5 + \gamma_5 D_c = 0$  and then  $m_q \rightarrow 0$  will make the pion mass to vanish without any non-zero  $m^{\text{cri}}$ .

**Results:** In this work, we use the 2+1+1 flavors (degenerate up and down, strange, and charm degrees of freedom) of highly improved staggered quarks (HISQ)

tag	$6/g^2$	$L$	$T$	$a(\text{fm})$	$c_{\text{sw}}$	$m_q^{\text{w}}a$	$c'_{\text{sw}}$	$m_q^{\text{w}'}a$	$m_q^{\text{ov}}a$	tag	$6/g^2$	$L$	$T$	$a(\text{fm})$	$m_q^{\text{ov}}a$
HISQ12	3.60	24	64	0.1213(9)	1.0509	-0.0695	1.31	0.010	0.015	DW11	2.13	24	64	0.1105(3)	0.015
HISQ09	3.78	32	96	0.0882(7)	—	—	—	—	0.011	DW08	2.25	32	64	0.0828(3)	0.011
HISQ06	4.03	48	144	0.0574(5)	1.0349	-0.0398	1.25	0.0014	0.008	DW06	2.37	32	64	0.0627(3)	0.008
HISQ03	4.37	96	288	0.0318(3)	1.0287	-0.0333	1.26	0.0030	—						

tag	$6/g^2$	$L$	$T$	$a(\text{fm})$	$c_{\text{sw}}$	$m_q^{\text{w}}a$	tag	$6/g^2$	$L$	$T$	$a(\text{fm})$	$c_{\text{sw}}$	$m_q^{\text{w}}a$
CLS10	3.34	24	48	0.0980(12)	2.06686	-0.3437	CLS08	3.40	32	96	0.0854(10)	1.98625	-0.3468
CLS06	3.55	48	128	0.0644(08)	1.82487	-0.3525	CLS04	3.85	64	192	0.0390(06)	1.61281	-0.3478

TABLE I. Setup of the ensembles, including the bare coupling constant  $g$ , lattice size  $L^3 \times T$  and lattice spacing  $a$ .  $m_q^{\text{w}}$  and  $m_q^{\text{w}'}$  are the bare quark masses using the clover fermion action with two clover coefficient  $c_{\text{sw}}$  and  $c'_{\text{sw}}$  respectively, and  $m_q^{\text{ov}}$  is the bare quark mass of the overlap fermion. The pion masses in all the cases are in the range of 310-360 MeV.

and one-loop Symanzik improved gauge ensembles from the MILC Collaboration [21] at four lattice spacings, 2+1 flavor domain wall (DW) quarks and Iwasaki gauge ensembles from the RBC/UKQCD collaboration [22] at three lattice spacings, and also 2+1 flavor clover quark and Luescher-Weisz (equivalent to Symanzik) gauge ensembles from CLS collaboration [23]. With 1-step HYP smearing [24] is applied on the MILC/RBC gauge configurations, we use  $\rho = 1.5/a$  for the overlap fermion, and two choices of the clover coefficients for the clover action: one is the tadpole improved tree level coefficient  $c_{\text{sw}}$  which is very close to one after the configuration is HYP smeared, and the other one  $c'_{\text{sw}} \sim 1.3$  to make the critical quark mass  $m_q^{\text{cri}}$  to be around zero. Thus one can see that the bare overlap quark mass  $m_q^{\text{ov}}a$  is roughly proportional to the lattice spacing if we require the pion mass to be around 310 MeV, but  $m_q^{\text{w}}a$  are always negative with  $c_{\text{sw}} \sim 1$  until we enlarge  $c_{\text{sw}}$  to  $\sim 1.3$ . For the CLS configuration, we simply use the unitary setup (without any smearing in the quark and gluon actions) to process the clover fermion calculation. Since most of the CLS ensembles except CLS10 use the open boundary condition, and then we just use the 1/3 of the time slides in the middle of the lattice for the volume source used by RI/MOM renormalization constant.

For the RI/MOM renormalization constant we used in this work, we use the momentum  $p = 2\pi/L(5, 5, 0, 0)$  on the MILC ensembles and tune  $p_{x,y}$  on the RBC/UKQCD ensembles to make  $\mu = \sqrt{p^2}$  to be roughly the same on all the ensembles within 6%. As shown in Fig. 1 for the ratio of the renormalization constants,

$$R_{\text{RI/MOM}}(z, \mu, \mu') = Z(z, \mu)/Z(z, \mu'), \quad (9)$$

with  $\mu' = \sqrt{-(p')^2} \sim 1.8$  GeV and  $p' = 2\pi/L(3, 3, 0, 0)$  on the MILC ensembles using different valence fermion actions and lattice spacings, the ratio just changes about 2% at  $z=1$  fm regardless the actions and lattice spacings, and then the systematic uncertainty from a 6% difference in  $\mu$  can be smaller than the statistical uncertainty. On the other hand, such a good convergence at small lattice spacing suggests that the UV divergence due to the discretized fermion actions can be perfectly cancelled up to the discretization errors. However, small residual  $z$  dependence may indicate some nonperturbative effect

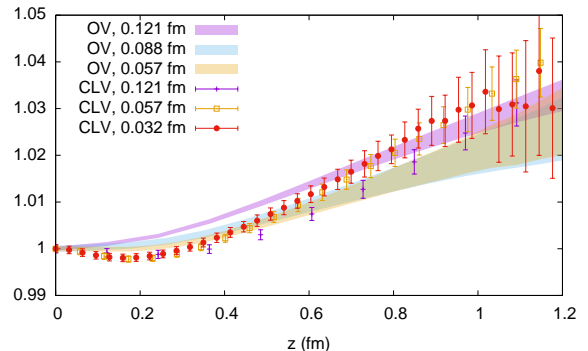


FIG. 1. The  $z$ -dependent ratio  $R_{\text{RI/MOM}}(z, \mu, \mu')$  defined in Eq. (9) between  $\mu \simeq 3\text{GeV}$  and  $\mu' \simeq 1.8$  GeV using the given valence action and lattice spacing on the MILC ensembles. The results with clover and overlap actions converge to the same limit at small lattice spacing. Note that the  $z$  dependence is weak but doesn't vanish.

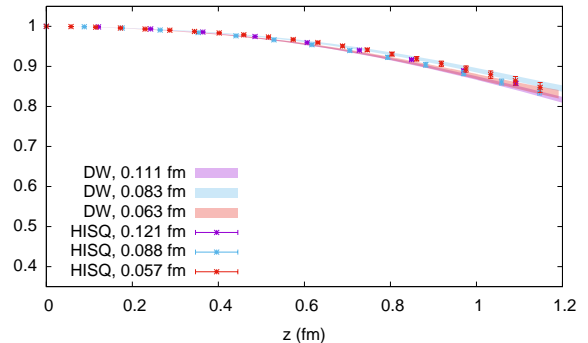


FIG. 2. RI/MOM renormalized pion matrix element using the overlap fermion on DW (bands) and also HISQ (data points) configurations. All the cases shows good agreement within  $\sim 1\%$  percent difference.)

in  $Z(z, \mu)$ . More informations of the linear divergence coefficients in different cases can be found in the supplementary materials [25].

Then we apply the renormalization constant at RI/MOM  $\mu=3.0(2)$  GeV to  $h_{\pi,\gamma_t}(z, a)$ , starting from the overlap case. As in Fig. 2, the renormalized pion matrix

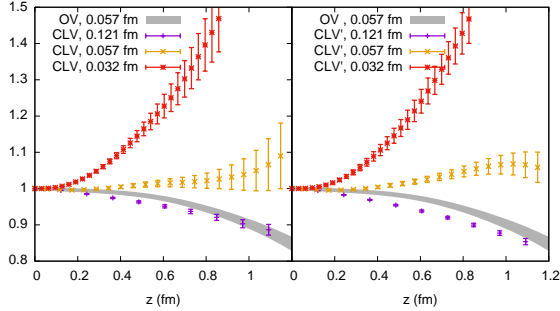


FIG. 3. Same as Fig 2, the cases using the clover fermion on HISQ configurations at different lattice spacings (data points), comparing to the overlap case (purple band). The left and right panels show the cases with  $c_{\text{sw}} \sim 1$  and 1.3 respectively. The residual linear divergence is conspicuous in the clover case with  $a \leq 0.06$  fm.

element  $h_{\pi,\gamma_t}^r(z, a)$  on different ensembles with different sea quark, gauge actions and lattice spacings are consistent with each other within  $\sim 1\%$  difference and doesn't show any obvious lattice spacing dependence. The data on different ensembles can have 2-3  $\sigma$  deviation based on their tiny statistical uncertainty at 0.5% level; such a deviation can be the systematic uncertainty coming from the mismatch in the pion mass, renormalization scale, finite volume and etc. The  $z$  dependence of  $h_{\pi,\gamma_t}(z, a)$  can be considered as the non-perturbative power corrections; and the fit gives  $\lambda_1 = -(0.067(4) \text{ GeV})^2$  and  $\lambda_2 = (0.15(14) \text{ GeV})^4$  in the range of  $z \in [0.0, 1.2]$  fm with  $\chi^2/\text{d.o.f.} \sim 1$ , if we use a simple  $1 + \sum_{i=1,2} \lambda_i z^{2i}$  form to describe the data and consider the data on different ensembles as independent samples. Both  $\lambda_{1,2}$  are at the order of  $\Lambda_{QCD}^n$  and it is consistent with the naive power counting.

In the clover fermion case, the RI/MOM renormalized  $h_{\pi,\gamma_t}^r(z, a)$  can have a very strong lattice spacing dependence, and such a dependence becomes even stronger at smaller lattice spacing. As in the left panel of Fig. 3, the changes in  $h_{\pi,\gamma_t}^r(z, a)$  from  $a = 0.057$  fm to 0.032 fm is much larger than that from  $a = 0.121$  fm to 0.057 fm, and the difference becomes exponentially larger with a bigger Wilson link length  $z$ . Such a behavior can be explained by a residual linear divergence which is not fully cancelled by  $Z(z, \mu)$ . If we change the clover coefficient by  $\sim 20\%$  and then reduce the critical quark mass to  $\mathcal{O}(0.01)$ , the lattice spacing dependence behavior is still the same as in the right panel of Fig. 3. More figures without HYP smearing on the Wilson link are provided in the supplementary materials [25], while all the conclusions here are basically unchanged.

Since  $m_q^{\text{cri}}$  is very sensitive to whether the gauge configuration used in the clover fermion action is HYP smeared, and the clover on HISQ setup can suffer from  $\mathcal{O}(a)$  mixed action effects, we also provide the unitary clover fermion case using the CLS ensembles in Fig. 4 without HYP

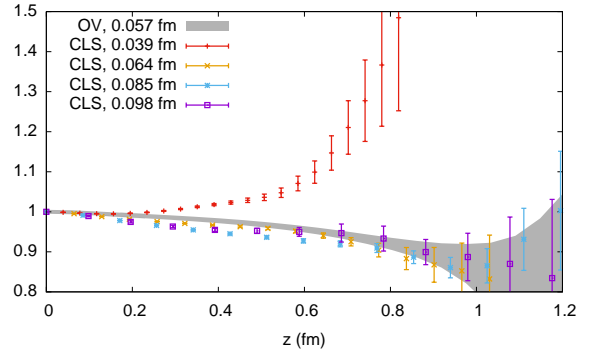


FIG. 4. Same as Fig 3, the cases of the unitary clover valence on clover sea with CLS ensembles (data points), comparing to to the overlap case (gray band). Note that the Wilson link is not HYP smeared for both the clover and overlap cases.

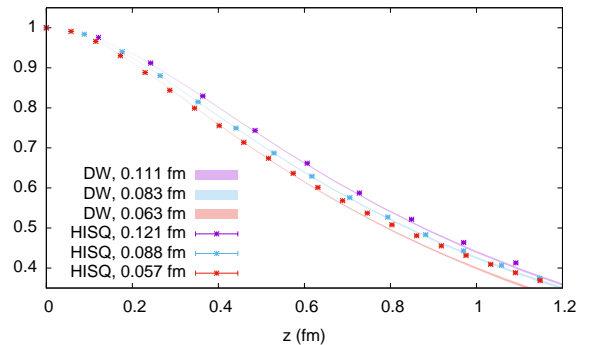


FIG. 5. The same as Fig. 2 but with the scalar current and corresponding RI/MOM renormalization, using the overlap fermion. The  $z$  dependence is stronger than the vector current case but still  $\mathcal{O}(\Lambda_{QCD}^2 z^2)$ .

smearing on either the fermion action or Wilson link. The situation seems to be better except the smallest lattice spacing, but the results at given  $z$  still increases on  $1/a$  except the case at largest lattice spacing which suffers from obvious discretization error.

By definition, the operator product expansion of  $h_\pi(z, a)$  includes the trace terms like  $\bar{\psi}\gamma_t D^2\psi$ , which equals to  $m^2\bar{\psi}\gamma_t\psi$  with the chiral fermion and would introduce the  $z$  dependence in Fig. 2; but  $\bar{\psi}\gamma_t D^2\psi$  using the clover fermion action would have additional linear divergence from the Wilson, clover and residual mass terms. Those unphysical terms could bring in additional linear divergences which may not be caught by the RI/MOM renormalization.

At the end of this section, we present the overlap pion matrix element with the scalar current instead of the vector one in Fig. 5. One can see that the lattice spacing dependence is much larger than the vector case, and we have to use the form  $1 + \sum_{i=1,2,3} \lambda_i z^{2i}$  with higher order correction to describe the data at  $a \simeq 0.06$  fm with  $\lambda_1 = -(0.241(4)(5) \text{ GeV})^2$ ,  $\lambda_2 = (0.212(4)(7) \text{ GeV})^4$  and  $\lambda_3 = -(0.172(4)(9) \text{ GeV})^6$ , where the second uncertainty

comes from the difference between the fitting parameters with MILC and RBC ensembles. Again, all the coefficients are at the order of  $\Lambda_{QCD}^{2n}$ . Note that the parameterizations for the vector and scalar matrix elements are not the only possibility to describe the data, and it just targets to a simple way to reconstruct our result for further studies.

We skipped the clover action case with the scalar current since it is similar to the vector case and the scalar current with the clover fermion is known to be more problematic due to the chiral symmetry breaking effect introduced by  $m^{cri}$ .

**Summary:** We have demonstrated that the linear divergence in the quark quasi-PDF proposed in LaMET framework can be properly eliminated using the RI/MOM renormalization, with the chiral fermion in this simplest case. It paves the way to a systematic study on PDF through the quasi-PDF approach, and also provides a solid numerical check on the factorization theorem of the quasi-PDF matrix elements. The corrections are  $\mathcal{O}(\Lambda_{QCD}^2 z^2)$ , while the effect using the vector current, is much smaller than that using the scalar current.

Our results also show clear evidences that there are residual linear divergences in the RI/MOM renormalized pion matrix element  $h_{\pi,\gamma_t}^R$  when the clover action is used for the valence quark, on the dynamical configurations with different quark and gluon actions, and it is irrelevant to the mixed action effect. The residual linear divergence is small when the lattice spacing is around 0.1 fm, but becomes very conspicuous at small lattice spacing likes 0.04 fm or so. Thus it is essential to check other

actions with the relatively good chiral symmetry like the domain wall fermion, and the ones with partly the chiral symmetry like the twisted mass fermion. If so, one can make a solid conclusion on the proper quark action that can be used in the quasi-PDF calculation, and answer whether the residual linear divergence in  $h_{\pi}^R$  is related to the explicit chiral symmetry breaking in the fermion action or not.

## ACKNOWLEDGEMENT

We thank the CLS, MILC and RBC/UKQCD collaborations for providing us their gauge configurations, and Long-Cheng Gui, Xiangdong Ji, Keh-Fei Liu, Andreas Schaefler, Wei Wang and Jian-Hui Zhang, Yong Zhao for useful information and discussion. The calculations were performed using the Chroma software suite [26] with QUDA [27–29] and GWU-code [30, 31] through HIP programming model [32]. The numerical calculation is supported by Strategic Priority Research Program of Chinese Academy of Sciences, Grant No. XDC01040100, and also HPC Cluster of ITP-CAS, Jiangsu Key Lab for NSLSCS. P. Sun is supported by Natural Science Foundation of China under grant No. 11975127, as well as Jiangsu Specially Appointed Professor Program. Y. Yang is supported by Strategic Priority Research Program of Chinese Academy of Sciences, Grant No. XDB34030303 and XDC01040100.

- 
- [1] X. Ji, Phys. Rev. Lett. **110**, 262002 (2013), arXiv:1305.1539 [hep-ph].
  - [2] X. Ji, Sci. China Phys. Mech. Astron. **57**, 1407 (2014), arXiv:1404.6680 [hep-ph].
  - [3] Y.-Q. Ma and J.-W. Qiu, Phys. Rev. **D98**, 074021 (2018), arXiv:1404.6860 [hep-ph].
  - [4] Y.-Q. Ma and J.-W. Qiu, Phys. Rev. Lett. **120**, 022003 (2018), arXiv:1709.03018 [hep-ph].
  - [5] T. Izubuchi, X. Ji, L. Jin, I. W. Stewart, and Y. Zhao, Phys. Rev. **D98**, 056004 (2018), arXiv:1801.03917 [hep-ph].
  - [6] C. Alexandrou, K. Cichy, M. Constantinou, K. Hadjiyiannakou, K. Jansen, H. Panagopoulos, and F. Steffens, Nucl. Phys. **B923**, 394 (2017), arXiv:1706.00265 [hep-lat].
  - [7] G. Martinelli, C. Pittori, C. T. Sachrajda, M. Testa, and A. Vladikas, Nucl. Phys. **B445**, 81 (1995), arXiv:hep-lat/9411010 [hep-lat].
  - [8] X. Ji and J.-H. Zhang, Phys. Rev. **D92**, 034006 (2015), arXiv:1505.07699 [hep-ph].
  - [9] X. Ji, J.-H. Zhang, and Y. Zhao, Phys. Rev. Lett. **120**, 112001 (2018), arXiv:1706.08962 [hep-ph].
  - [10] T. Ishikawa, Y.-Q. Ma, J.-W. Qiu, and S. Yoshida, Phys. Rev. **D96**, 094019 (2017), arXiv:1707.03107 [hep-ph].
  - [11] J. Green, K. Jansen, and F. Steffens, Phys. Rev. Lett. **121**, 022004 (2018), arXiv:1707.07152 [hep-lat].
  - [12] M. Constantinou and H. Panagopoulos, Phys. Rev. **D96**, 054506 (2017), arXiv:1705.11193 [hep-lat].
  - [13] J.-W. Chen, T. Ishikawa, L. Jin, H.-W. Lin, Y.-B. Yang, J.-H. Zhang, and Y. Zhao, Phys. Rev. **D97**, 014505 (2018), arXiv:1706.01295 [hep-lat].
  - [14] I. W. Stewart and Y. Zhao, Phys. Rev. **D97**, 054512 (2018), arXiv:1709.04933 [hep-ph].
  - [15] C. Alexandrou, K. Cichy, M. Constantinou, J. R. Green, K. Hadjiyiannakou, K. Jansen, F. Manigrasso, A. Scapellato, and F. Steffens, (2020), arXiv:2011.00964 [hep-lat].
  - [16] H.-W. Lin, J.-W. Chen, and R. Zhang, (2020), arXiv:2011.14971 [hep-lat].
  - [17] Y.-S. Liu *et al.* (Lattice Parton), Phys. Rev. **D101**, 034020 (2020), arXiv:1807.06566 [hep-lat].
  - [18] P. H. Ginsparg and K. G. Wilson, Phys. Rev. **D25**, 2649 (1982).
  - [19] T.-W. Chiu, Phys. Rev. **D60**, 034503 (1999), arXiv:hep-lat/9810052 [hep-lat].
  - [20] K.-F. Liu, Int. J. Mod. Phys. **A20**, 7241 (2005), arXiv:hep-lat/0206002 [hep-lat].
  - [21] A. Bazavov *et al.* (MILC), Phys. Rev. **D87**, 054505 (2013), arXiv:1212.4768 [hep-lat].

- [22] T. Blum *et al.* (RBC, UKQCD), Phys. Rev. **D93**, 074505 (2016), arXiv:1411.7017 [hep-lat].
- [23] M. Bruno *et al.*, JHEP **02**, 043 (2015), arXiv:1411.3982 [hep-lat].
- [24] A. Hasenfratz and F. Knechtli, Phys. Rev. **D64**, 034504 (2001), arXiv:hep-lat/0103029 [hep-lat].
- [25] Supplementary materials.
- [26] R. G. Edwards and B. Joo (SciDAC, LHPC, UKQCD), *Lattice field theory. Proceedings, 22nd International Symposium, Lattice 2004, Batavia, USA, June 21-26, 2004*, Nucl. Phys. Proc. Suppl. **140**, 832 (2005), [832(2004)], arXiv:hep-lat/0409003 [hep-lat].
- [27] M. A. Clark, R. Babich, K. Barros, R. C. Brower, and C. Rebbi, Comput. Phys. Commun. **181**, 1517 (2010), arXiv:0911.3191 [hep-lat].
- [28] R. Babich, M. A. Clark, B. Joo, G. Shi, R. C. Brower, and S. Gottlieb, in *SC11 International Conference for High Performance Computing, Networking, Storage and Analysis Seattle, Washington, November 12-18, 2011* (2011) arXiv:1109.2935 [hep-lat].
- [29] M. A. Clark, B. Jo, A. Strelchenko, M. Cheng, A. Gambhir, and R. Brower, (2016), arXiv:1612.07873 [hep-lat].
- [30] A. Alexandru, C. Pelissier, B. Gamari, and F. Lee, J. Comput. Phys. **231**, 1866 (2012), arXiv:1103.5103 [hep-lat].
- [31] A. Alexandru, M. Lujan, C. Pelissier, B. Gamari, and F. X. Lee, in *Proceedings, 2011 Symposium on Application Accelerators in High-Performance Computing (SAAHPC'11): Knoxville, Tennessee, July 19-20, 2011* (2011) pp. 123–130, arXiv:1106.4964 [hep-lat].
- [32] Y.-J. Bi, Y. Xiao, M. Gong, W.-Y. Guo, P. Sun, S. Xu, and Y.-B. Yang, *Proceedings, 37th International Symposium on Lattice Field Theory (Lattice 2019): Wuhan, China, June 16-22 2019*, PoS **LATTICE2019**, 286 (2020), arXiv:2001.05706 [hep-lat].

## SUPPLEMENTAL MATERIALS

### A. fitting the renormalization constant

Since different quark flavors, quark and gauge actions used by MILC and RBC/UKQCD makes their bare coupling to be differ by a factor  $\sim 1.7$  at similar lattice spacing, we consider the fit form

$$Z(z; a) = Z_0(a) \exp \left\{ \frac{\alpha_s(a)}{\alpha_s(a_0)} \left[ \left( \frac{m_{-1}}{a} + m_0 \right) z + d_1 z \log \left( \frac{z}{z_0} \right) \right] \right\}, \quad (10)$$

where  $z_0=0.3$  fm and  $a_0=0.1$  fm. We also introduce a dummy systematic uncertainty factor  $\delta_{sys}$  to enlarge the uncertainty of the renormalization constants into  $\sqrt{(\delta Z)^2 + \delta_{sys}^2 Z^2}$ , as the statistical uncertainty at small  $z$  can smaller than kinds of the systematic uncertainty from discretization, partially quenching, lattice spacing determination, valence/sea quark mass and volume dependence.

Sea	HISQ+S			DW+I	CLV+S
Valence	OV	CLV	CLV'	OV	CLV
$m_{-1}$	0.215(2)	0.239(3)	0.245(5)	0.221(3)	0.240(4)
$\delta_{sys}(\%)$	0.006	0.013	0.024	0.008	0.013

TABLE II. The linear divergence parameters we obtained with the parameterization in Eq. (10) using  $a_0=0.1$  fm and  $z_0=0.3$  fm. ‘‘S’’ means the Symanzik gauge action and ‘‘I’’ is used for the Iwasaki gauge action.

Then we fit the renormalization constant in the range  $z \in [0.2, 1.2]$  fm with the same actions but at different lattice spacings, and tune the  $\delta_{sys}$  to ensure  $\chi^2/d.o.f \sim 1$  and p-value  $\geq 0.05$ . The values in different cases are summarized in Table II. We can see that the  $m_{-1}$  are  $\sim 0.2$  for all the cases, while the  $\delta_{sys}$  in the unitary clover case is larger than the other cases, and the major difference is that the HYP smearing is applied on the valence fermion actions in all other cases.

### B. HYP smearing dependence for the overlap fermion

Fig. 6 compares the RI/MOM renormalized the pion matrix element with the vector current  $h_{\pi, \gamma_t}(z, a)$ , using overlap fermion with and without HYP smearing on the Wilson link. The results just differ by less the 1% while the cases without HYP smearing have larger statistical uncertainties. Such a difference can come from systematic uncertainties of the mismatch of the pion mass, mixed action effect and etc.

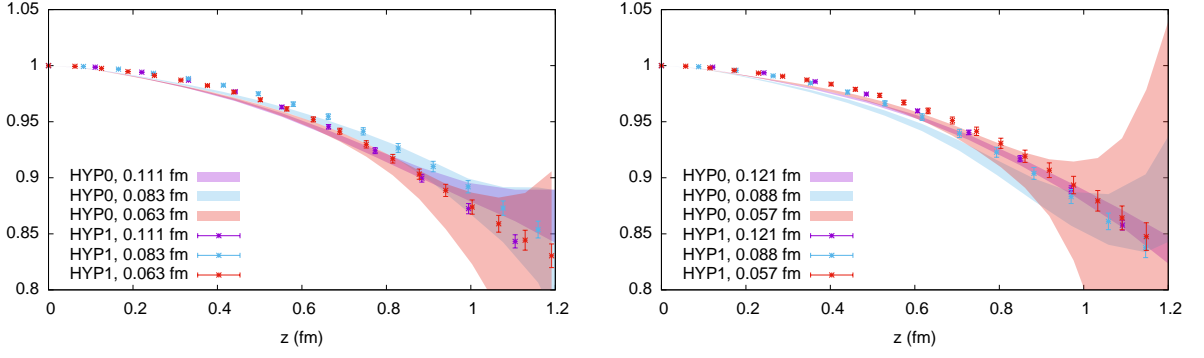


FIG. 6. The RI/MOM renormalized pion matrix element with the vector current, using the overlap fermion on RBC ensembles (left panel) and MILC ensembles (right panel). The data points correspond to the cases with 1-step of the HYP smearing, and the bands are the cases without HYP smearing on the Wilson link.

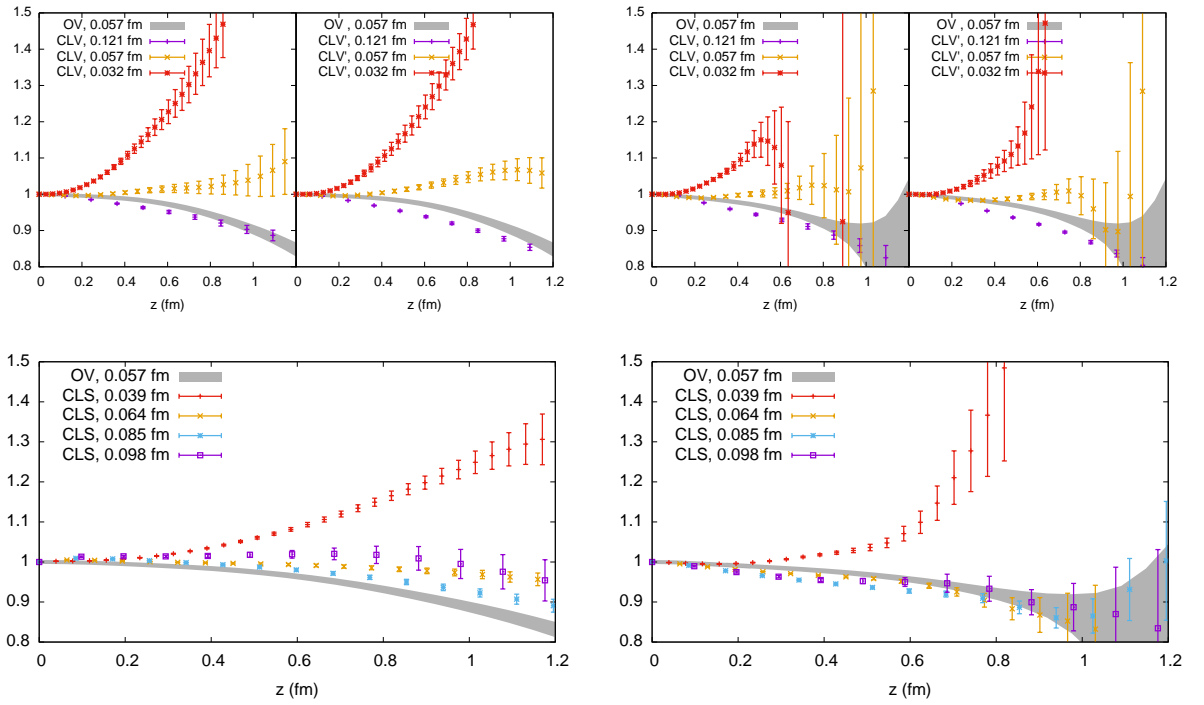


FIG. 7. The RI/MOM renormalized pion matrix element with the vector current, using the clover fermion on MILC ensembles (upper panels) and CLS ensembles (lower panel), with (left panels) and without (right panels) HYP smearing. The residual linear divergences are always exist.

### C. HYP smearing dependence for the clover fermion

Fig. 7 compares the cases with and without HYP smearing on the Wilson link, for the RI/MOM renormalized the pion matrix element  $h_{\pi, \gamma_t}(z, a)$ , using the clover fermion. The upper two panels are the cases using the clover fermion on the MILC ensembles (the gauge link in the clover action is HYP smeared, and such a case has  $\mathcal{O}(a)$  mixed action effect), and lower two panels are the cases using the clover fermion on CLS ensembles (the gauge link in the clover action is the original one, and it is a unitary case without any mixed action effect). The left two panels apply the HYP smearing on the Wilson link, but the right two panels are not. Note that the overlap results shown in the gray band uses the HYP smearing in left two panels but not in right two panels, to provide a fair comparison even though their difference are smaller than 1%. The linear divergences are obvious for all the simulation setups using the clover fermion, and we can see that the behavior of  $h_{\pi, \gamma_t}(z, a)$  is sensitive to whether the HYP smearing is applied on the

Wilson link, even though the dependence is weakened when the HYP smearing is applied on the gauge link in the clover action. It is consistent with our suspicion that the residual linear divergence is directly related to the clover action itself.

---